Background and target randomization and Root Mean Square (RMS) background matching using a new ΔT metric definition

Howard C. Choe

Battelle Memorial Institute
Avionics/Vetronics Systems and Technology
Columbus, Ohio 43201-2693

Thomas Meitzler and Grant Gerhart

Research Branch/AMSTA-JA
The U.S. Army Tank Automotive Research,
Development and Engineering Center (TARDEC)
Warren, Michigan 48397-5000

ABSTRACT

EO/IR/Laser detection of a target amidst clutter/background is a difficult problem often treated with simplistic models. Unlike noise, clutter is more complex, neither spectrally white nor statistically Gaussian. Therefore, it is insufficient to lump clutter with noise and use standard detection curves. Using current target detection models, it is extremely difficult to perform effectiveness assessments of signature management technologies for survivability of military ground vehicles. Current models do not consider the vehicle on a component-level basis and do not account for artifacts introduced into images from aliasing and varying amounts of clutter. Algorithms must be developed that quantify the effects of random backgrounds on the imaging capability of electro-optical systems to improve false alarm rates. Current trends dictate that EO/IR/Laser imaging systems must consider developments in signature management technologies and countermeasures that are driving clutter magnitudes higher than target signature magnitudes. These trends make the problem of target detection in clutter especially critical. Battelle has produced image randomization software called BATRAN (Background and Target Randomization) which computes various types of statistical distributions to randomize background and target pixels separately. The types of statistics implemented include exponential, Gaussian, log-normal, and Rice distributions for both the background and target. To generate synthetic images to assess the detection performance of thermal imaging systems and countermeasured platform signatures, a method to characterize the background and target is required so that their signatures can be statistically matched. Current methods use an area-weighted average temperature difference (AWAΔT), which is regarded as inadequate in representing observer's sensitivity to the inherent detection cues of the target/background/clutter signatures. In an effort to identify a more robust and accurate ΔT metric definition for background and target matching, Battelle also developed a new ΔT metric definition and its equation using RMS pixel-based higher order statistics for the background and target signature pixel data in a scene image. This new ΔT metric provides a better estimate of true signature difference between the background/clutter and target, enabling more accurate matching of the background/clutter and target for use in sensor detection performance assessment.

1. INTRODUCTION

BATRAN, a software package produced by Battelle, randomizes each background and target pixel in an input scene image. The randomizing distribution of the background and target pixels can be different. The properties of randomizing statistical distributions are provided as *a priori* distributions. A method to randomize pixels in an image is also provided. Output images from BATRAN are presented along with inherent input images. The output images are randomized with various pairs of randomizing distributions. These output images are then used for ΔT analysis.

Currently used ΔT metric definitions and their equations[1,2,3] are not proper representations for describing temperature varying features of a target and/or its background. Some ΔT metrics oversimplify the effects of these features and misrepresent the apparent temperature difference which provides an inherent detection cue of target/background/clutter. Other ΔT metrics treat the pixels from a target and its background in a sensor image as if they come from two separate images, which ignores a relative temperature apparentness of the target and its background. These facts inadequately represent a human observer's sensitivity to the detection of target from background and clutter. Therefore, these problems associated with the currently used ΔT metrics necessitate the development of a new ΔT metric

Report Documentation Page

Form Approved
OMB No. 0704-0188

1. REPORT DATE	2. REPORT TYPE	3. DATES COVERED
17 MAY 1993	**N/A**	**-**

4. TITLE AND SUBTITLE	5a. CONTRACT NUMBER
Background and target randomization Root Mean Square (RMS) background matching using a new delta T metric definition	5b. GRANT NUMBER
	5c. PROGRAM ELEMENT NUMBER
6. AUTHOR(S)	5d. PROJECT NUMBER
Howard C. Choe; Thomas Meitzler; Grant Gerhart	5e. TASK NUMBER
	5f. WORK UNIT NUMBER
7. PERFORMING ORGANIZATION NAME(S) AND ADDRESS(ES)	8. PERFORMING ORGANIZATION REPORT NUMBER
US Army RDECOM-TARDEC 6501 E 11 Mile Rd Warren, MI 48397-5000	**18746**
9. SPONSORING/MONITORING AGENCY NAME(S) AND ADDRESS(ES)	10. SPONSOR/MONITOR'S ACRONYM(S)
	TACOM/TARDEC
	11. SPONSOR/MONITOR'S REPORT NUMBER(S)
	18746

12. DISTRIBUTION/AVAILABILITY STATEMENT
Approved for public release, distribution unlimited

13. SUPPLEMENTARY NOTES

14. ABSTRACT

15. SUBJECT TERMS

16. SECURITY CLASSIFICATION OF:			17. LIMITATION OF ABSTRACT	18. NUMBER OF PAGES	19a. NAME OF RESPONSIBLE PERSON
a. REPORT	b. ABSTRACT	c. THIS PAGE			
unclassified	**unclassified**	**unclassified**	**SAR**	**14**	

definition and its equation. In this paper, a new ΔT metric is defined. An equation representing this new definition is then derived. This new ΔT equation is implemented in BATRAN along with other ΔT equations with which the new ΔT metric is compared.

The remainder of this paper is organized as follows: Section 2 discusses the theory of the background and target randomization algorithm implemented in BATRAN including the *a priori* distributions and the pixel randomization method, and presents the randomized output images; Section 3 discusses the new ΔT definition and its equation derivation, and compares the new ΔT metric with other ΔT metrics; Summary and conclusions are given in Section 4; Section 5 contains acknowledgements; and, Section 6 lists the references cited during this research performance period.

2. BACKGROUND/CLUTTER AND TARGET STATISTICS MODELING FOR RANDOMIZATION

This section discusses the theory behind the background and target pixel randomization algorithm and its development and modeling in BATRAN. The various statistical distributions available for the background and target randomization are provided by their probability density function (PDF) and cumulative distribution function (CDF). The random number generation from a desired statistical distribution using the inverse transform method is presented. To assure that the generated random numbers represent the desired statistics, BATRAN-simulated PDF and CDF are compared to the calculated (or exact) PDF and CDF. Finally, the BATRAN-randomized output images are displayed to show effects of the randomization by different statistics on a couple of input inherent images.

2.1 Properties of *a priori* distributions

The statistical distributions available for image randomization in BATRAN are exponential, Gaussian, log-normal, and Rice. Because these distributions are not derived from a physical description of clutter, they are referred to as *a priori* distributions. These are expressed by a PDF and a CDF, denoted by $p(x)$ and $P(x)$, respectively. For *a priori* distribution equations presented, μ and σ denote the mean and standard deviation of the distribution, respectively. Another parameter provided for the log-normal and Rice distributions is the standard deviation-to-mean ratio, denoted by R.

2.1.1 Exponential distribution

The PDF and CDF of the exponential distribution are given in (1.a) and (1.b), respectively. $P(x)$ is the definite integral of $p(x)$, $P(x) = \int_{-\infty}^{x} p(\tau)\, d\tau$.

$$p(x) = \frac{1}{\mu}\exp\left(-\frac{x}{\mu}\right) \quad (a); \qquad P(x) = 1 - \exp\left(-\frac{x}{\mu}\right) \quad (b) \tag{1}$$

2.1.2 Gaussian distribution

The Gaussian PDF is given in (2).

$$p(x) = \frac{1}{\sqrt{2\pi}\sigma}\exp\left\{-\frac{(x-\mu)^2}{2\sigma^2}\right\} \tag{2}$$

Even though there is no analytic closed-form expression of the Gaussian CDF, it can be expressed by using the error function, $Z(x) = \frac{1}{\sqrt{2\pi}}\exp(-\frac{x^2}{2})$. Integrating $Z(x)$, the error function's CDF is obtained as indicated in (3).

$$P_Z(y) = \frac{1}{\sqrt{2\pi}}\int_{-\infty}^{y}\exp\left\{-\frac{\tau^2}{2}\right\}d\tau = \int_{-\infty}^{y} Z(\tau)\,d\tau \tag{3}$$

Applying (3) to (2), (4) gives the Gaussian CDF in terms of the error function's CDF, $P_Z(y)$.

$$P(x) = \frac{1}{\sqrt{2\pi}\sigma}\int_{-\infty}^{x}\exp\left\{-\frac{(\tau-\mu)^2}{2\sigma^2}\right\}d\tau = \frac{1}{\sqrt{2\pi}}\int_{-\infty}^{\frac{x-\mu}{\sigma}}\exp\left\{-\frac{\tau^2}{2}\right\}d\tau = P_Z\left(\frac{x-\mu}{\sigma}\right) \quad (4)$$

The Gaussian CDF can be then represented as in (5), which is the error function's CDF approximation. This equation is a polynomial and rational approximation[4].

$$P(x) = P_Z(\nu,t) = 1 - Z(\nu)(b_1 t + b_2 t^2 + b_3 t^3 + b_4 t^4 + b_5 t^5) + \epsilon(\nu) \quad (5)$$

where $\nu = \frac{x-\mu}{\sigma}$ and $t = \frac{1}{1+q\nu}$. The error term is bounded such that $|\epsilon(\nu)| < 7.5\times10^{-8}$. The coefficient values in (5) are $b_1 = 0.319381530$, $b_2 = -0.356563782$, $b_3 = 1.781477937$, $b_4 = -1.821255978$, $b_5 = 1.330274429$, and $q = 0.2316419$.

2.1.3 Log-normal distribution[5,6,7]

The PDF of the log-normal distribution is given in (6).

$$p(x) = \frac{1}{\sqrt{2\pi}\sigma_{\ln}x}\exp\left\{-\frac{[\log_e(x)-m_{\ln}]^2}{2\sigma_{\ln}^2}\right\} = \frac{1}{\sqrt{2\pi}\sigma_{\ln}x}\exp\left\{-\frac{1}{2\sigma_{\ln}^2}\left[\log_e\left(\frac{x}{m}\right)\right]^2\right\} \quad (6)$$

Since the log-normal distribution is a Gaussian distribution with the natural logarithm of random variables, (5) is used with $\nu = \frac{\log_e(x)-m_{\ln}}{\sigma_{\ln}}$ to obtain the log-normal CDF. This is because the log-normal CDF can be written as (7).

$$P(k) = \frac{1}{\sqrt{2\pi}}\int_{-\infty}^{\frac{\log_e x - m_{\ln}}{\sigma_{\ln}}}\exp\left(-\frac{k^2}{2}\right)dk = P_Z\left(\frac{\log_e x - m_{\ln}}{\sigma_{\ln}}\right) \quad (7)$$

Terms in (7) are $\sigma_{\ln} = \log_e(\sigma)$ = standard deviation of $\log_e\left(\frac{x}{m}\right)$, and $m_{\ln} = \log_e(m)$, where m is the median of x. The mean-to-median ratio ($M = \mu/m$) of x is related to the standard deviation as in (8).

$$\sigma_{\ln} = \left[2\times\log_e(M)\right]^{\frac{1}{2}} = \left[2\times\log_e\left(\frac{\mu}{m}\right)\right]^{\frac{1}{2}} = \left[2\times\{\log_e(\mu) - m_{\ln}\}\right]^{\frac{1}{2}} \quad (8)$$

The median can then be found by solving (8) when the mean and the standard deviation are given for the log-normal distribution as shown in (9).

$$m_{\ln} = \log_e(m) = \log_e(\mu) - \frac{\sigma_{\ln}^2}{2} \quad (9)$$

The standard deviation-to-mean ratio (R) is expressed in (10.a), which can be solved for the standard deviation when R is provided as indicated in (10.b).

$$R = \sqrt{e^{\sigma_{\ln}^2} - 1} \quad (a); \qquad \sigma_{\ln} = \sqrt{\log_e(R^2+1)} \quad (b) \quad (10)$$

2.1.4 Rice distribution[5,6]

The PDF of the Rice distribution is expressed in (11), where $I_0(\alpha)$ is the zero-order modified Bessel function of first kind. The standard deviation-to-mean ratio (R) is expressed in (12.a). When R is given, the dominant-to-diffuse ratio

(r) can be expressed as in (12.b). The dominant-to-diffuse ratio is the ratio of the single dominant scatterer signature to the total signature of the small scatterers.

$$p(x) = \frac{1+r}{\mu}\exp\left\{-r-(1+r)\frac{x}{\mu}\right\} I_0\left(\sqrt{r(1+r)\frac{x}{\mu}}\right) \tag{11}$$

$$R = \frac{\sqrt{1+2r}}{1+r} \quad (a); \qquad r = -g + \sqrt{g\times(g-1)} \quad (b); \qquad g = 1 - R^{-2} \quad (c) \tag{12}$$

Numerical integration of the Rice PDF is necessary to obtain its CDF because there is neither an analytic closed-form expression nor a polynomial approximation of the Rice CDF.

2.1.5 Distribution example

Figure 1 shows an example of the four distributions defined above. Shown is each distribution's complement cumulative probability (CCP), $1 - \int_{-\infty}^{x} p(\tau)d\tau$. Each distribution has a mean of 10^{-2}. The second parameter of each distribution is shown in Table 1.

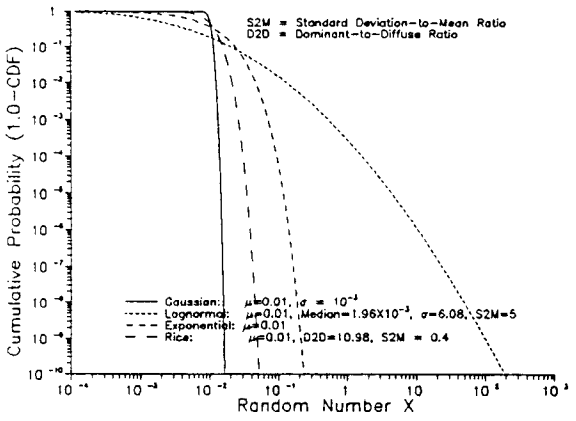

Figure 1 Example of cumulative distributions

Table 1. The value of the mean and the second parameter.

Distribution type	Mean	Second parameter	Input to BATRAN
Exponential	$\mu = 10^{-2}$	N/A	$\mu = 10^{-2}$
Gaussian	$\mu = 10^{-2}$	$\sigma = 10^{-3}$	$\sigma = 10^{-3}$
Log-normal	$\mu = 10^{-2}$ ($m = 1.96\times10^{-3}$ or $m_{ln} = -6.2343$)	$\sigma = 6.08$ (or $\sigma_{ln} = 1.805$)	$R = 5.0$
Rice	$\mu = 10^{-2}$	$r = 10.9782$	$R = 0.4$

2.2 Inverse transform method[8] (ITM) to randomize an input scene image

The inverse transform method is applied to generate random deviates (or random numbers) to randomize the background and target pixels using a desired distribution. This process is modeled in BATRAN. Figure 2 is used to illustrate the ITM implementation in BATRAN with the following steps.

Step 1: Generate a desired CDF either analytically or numerically, which is denoted by $P(x)$ and represented by a solid line in Figure 2.

Step 2: Generate uniform random deviates between 0 and 1, which is denoted by y.

Step 3: With $P(x)$ and y, one-to-one matching of y and x can be performed using $P(x)$ to obtain x, which is a random deviate from the desired distribution.

Applying ITM to an input (inherent) scene image, pixels are randomized with a desired statistical distribution. It is known that a pixel belongs either to the background or to the target prior to the randomization. Therefore, the background pixels can be randomized by one statistical distribution and the target pixels can be randomized by another distribution. The

random numbers, which may represent fluctuations in temperature, intensity, or radiance, are generated and added to the inherent background or target pixel values.

2.4 Comparison of exact distribution and the BATRAN generated distribution

In this section, random variates generated (or simulated) by BATRAN are examined to determine whether they closely follow the selected distribution by comparing them to the exact (or calculated) distribution. Figures 3, 4, 5, and 6 show the PDF for exponential, Gaussian, log-normal, and Rice distributions, respectively. Figures 7, 8, 9, and 10 show the CDF for exponential, Gaussian, log-normal, and Rice distributions, respectively. In each figure, the solid and dotted lines represent the calculated and simulated distributions, respectively. The simulated distribution is generated by performing 10^6 trials. From Figures 3, 4, 5, and 6, it is apparent that the number of trials to generate the simulated distribution is 10^6 since there are no samples taken beyond the PDF of 10^{-6}. It is also noted that as the simulated PDF approaches the tail region of the distribution, it deviates from the calculated PDF. This is because not enough samples are taken at each end of the tail regions to replicate the calculated PDF. However, the simulated CDF, as shown in Figures 7, 8, 9, and 10, agrees with the calculated CDF up to the complement cumulative probability (CCP) of 10^{-5}. Between the CCP of 10^{-5} and 10^{-6}, the simulated CDF deviates from the calculated CDF. Beyond the CCP of 10^{-6}, no data is available. Figures 3 and 7 show the exponential PDF and CDF, respectively. The mean (μ) of this distribution is 10. Figures 4 and 8 show the Gaussian PDF and CDF, respectively. The mean (μ) is 0 and the standard deviation (σ) is 20. Figures 5 and 9 show the log-normal PDF and CDF, respectively. The mean (μ) is 5 and the standard deviation-to-mean ratio (R) is 1. From the mean and the standard deviation-to-mean ratio, the median (m) and the standard deviation (σ) are 3.5355 and 2.2992, respectively, using (9) and (10.b). In natural logarithm, the median (m_{ln}) and the standard deviation (σ_{ln}) are 1.2629 and 0.8326, respectively. Figures 6 and 10 show the Rice PDF and CDF, respectively. The mean (μ) of the distribution is 35 and the standard deviation-to-mean ratio (R) is 0.5. From the standard deviation-to-mean ratio, the dominant-to-diffuse ratio (r) is 6.4641 using (12.b) and (12.c). These figures show that the random numbers generated in BATRAN closely follow the exact PDF and CDF. This not only verifies that the random numbers are generated with the input statistics parameters, but also validates that they are generated by the desired distribution.

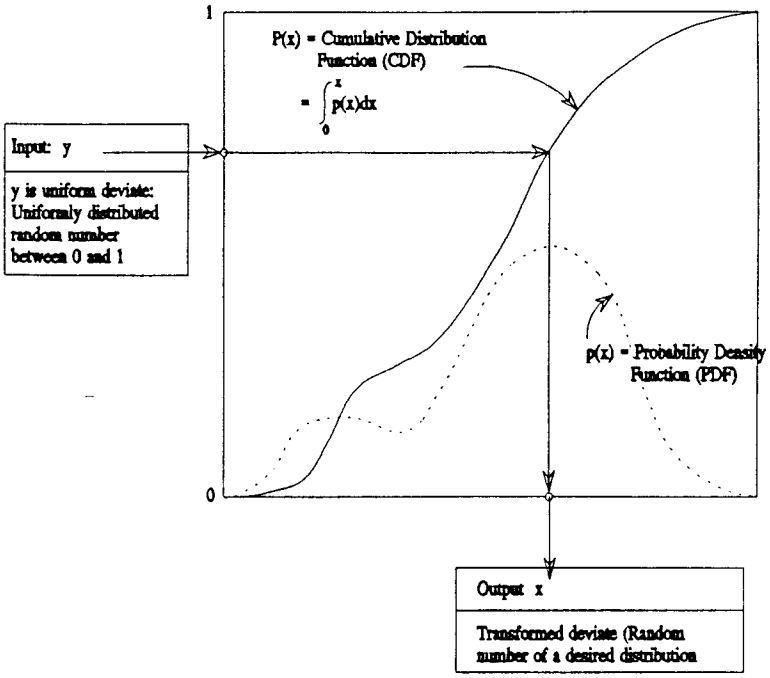

Figure 2 Illustration of inverse transform method (ITM)

2.5 Output images from BATRAN after background and target pixel randomization

Example output images from BATRAN after randomization were generated to demonstrate the effects of the randomization with various distributions. A simulated and a measured input inherent images were used for the randomization. The simulated inherent image is shown in Figure 11. The measured inherent image is shown in Figure 12. The simulated image was generated by the Wright Laboratories Tactical Decision Aid (TDA) model at Battelle. The measured image was provided by TARDEC. The size of the simulated and measured images were 378×377 and 512×512 pixels, respectively. Background pixel values of the simulated inherent image were set to zero; therefore, no difficulties arose in separating the background pixels from the target pixels. However, the measured image had to be

Probability density function (PDF): Calculated vs. Simulated

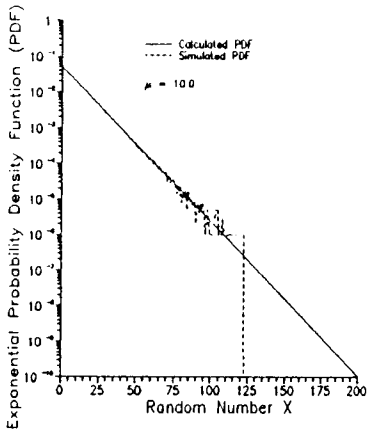

Figure 3 Exponential

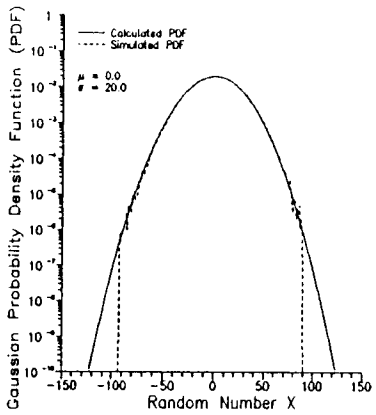

Figure 4 Gaussian

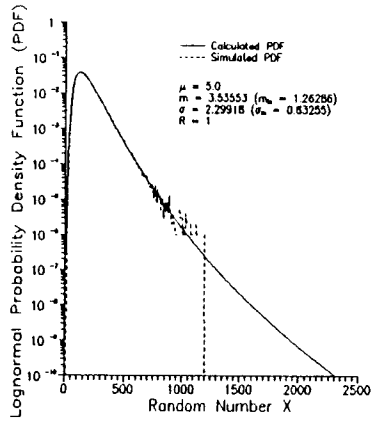

Figure 5 Log-normal

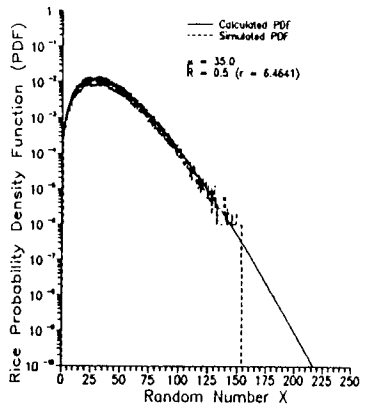

Figure 6 Rice

Cumulative distribution function (CDF) : Calculated vs. Simulated

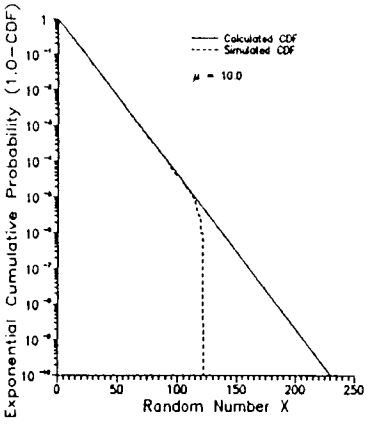

Figure 7 Exponential

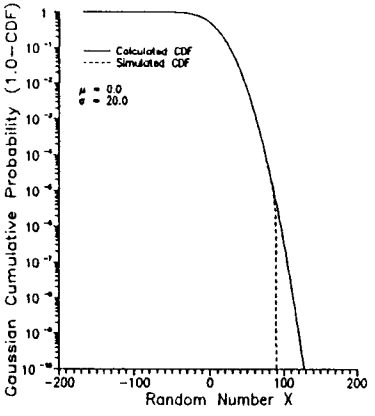

Figure 8 Gaussian

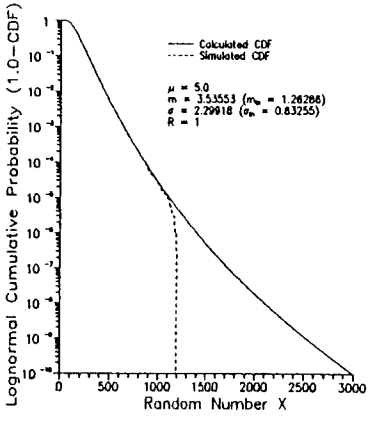

Figure 9 Log-normal

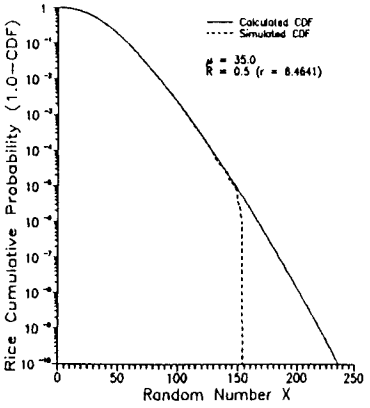

Figure 10 Rice

processed to separate the background pixels from the target pixels. The Geographic Resources Analysis Support System (GRASS) software package was used to cut out the target pixels from the background pixels. The output image file from GRASS also had the background pixels assigned to zero.

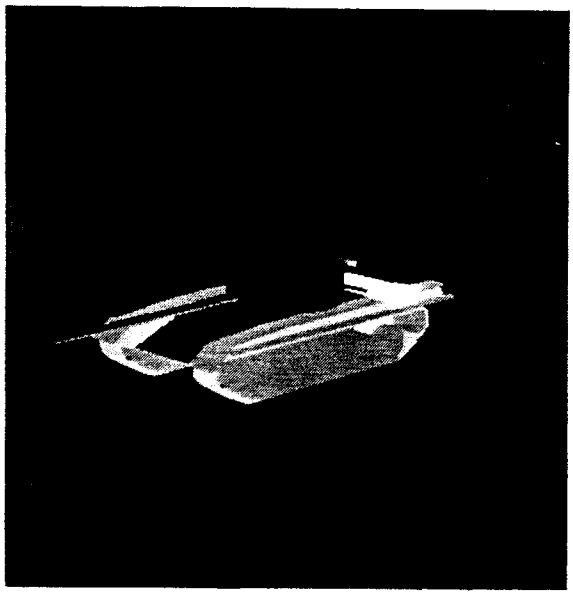

Figure 11 Simulated input inherent image.

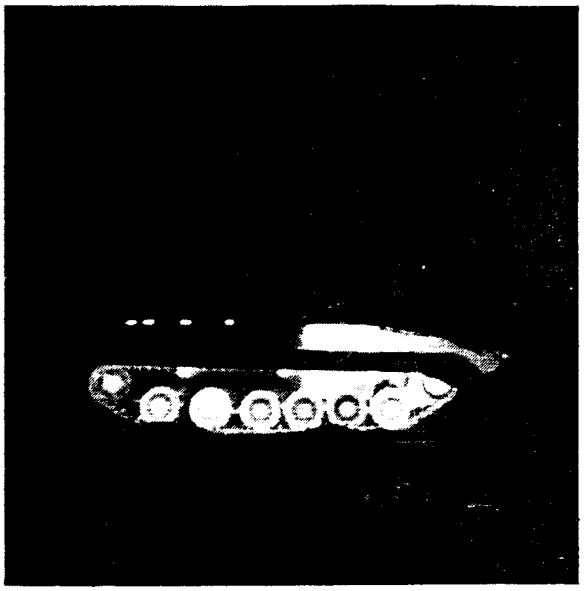

Figure 12 Measured input inherent image.

2.5.1 Output image examples with the simulated/measured image

For output images shown in Figures 13-16, Table 2 summarizes the types of statistical distributions and associated parameters used to randomize the simulated input inherent image. For output images shown in Figures 17-20, Table 3 summarizes the distributions and parameters used to randomize the measured input inherent image. The randomizing statistics for the target and background pixels are different for each randomized output image. These figures are discussed in detail using various ΔT metric definitions in Section 3.3

Table 2 Randomization parameters of BATRAN output image using the simulated input inherent image.

Simulated Image	Background Pixel Randomizing Statistics		Target Pixel Randomizing Statistics	
Figure #	Distribution Type	Distribution Parameters	Distribution Type	Distribution Parameters
13	Exponential	$\mu = 10$	Gaussian	$\mu=0$; $\sigma=10$
14	Gaussian	$\mu=24.45;\sigma=5$	Exponential	$\mu = 5$
15	Log-normal	$\mu = 6$; $R = 1$ $m_{ln} = 1.4452$ $\sigma_{ln} = 0.8326$	Rice	$\mu=1$; $R=0.5$ $r = 6.4641$
16	Rice	$\mu=15$; $R=1$ $r = 0$	Log-normal	$\mu=12$;$R=0.95$ $m_{ln}=2.1633$ $\sigma_{ln}=0.8020$

Table 3 Randomization parameters of BATRAN output image using the measured input inherent image.

Measured Image	Background Pixel Randomizing Statistics		Target Pixel Randomizing Statistics	
Figure #	Distribution Type	Distribution Parameter	Distribution Type	Distribution Parameter
17	Exponential	$\mu = 25$	Log-normal	$\mu = 7$; $R = 1$ $m_{ln} = 1.5993$ $\sigma_{ln} = 0.8326$
18	Gaussian	$\mu = 10$ $\sigma = 10$	Rice	$\mu=10$; $R=0.5$ $r = 6.4641$
19	Log-normal	$\mu=10$; $R=0.9$ $m_{ln}=2.0059$ $\sigma_{ln}=0.7703$	Gaussian	$\mu = 7$; $\sigma=10$
20	Rice	$\mu=34$;$R=0.95$ $r = 0.45401$	Exponential	$\mu = 30$

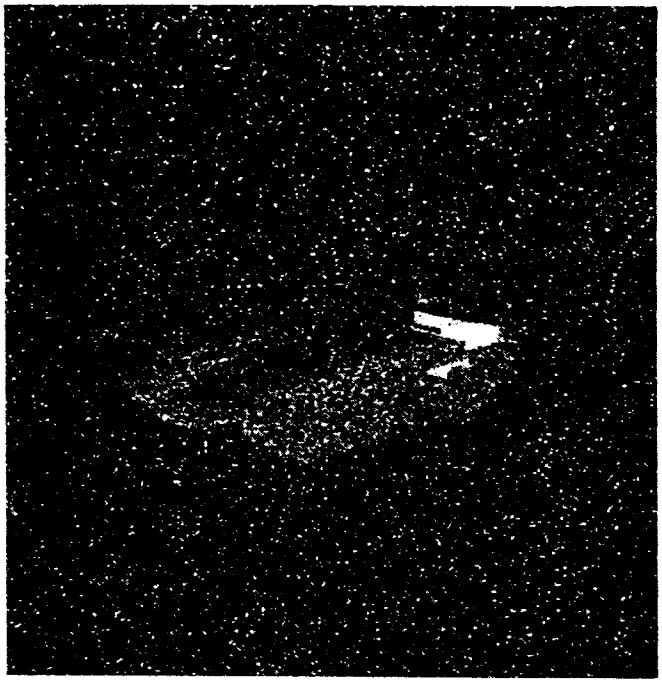

Figure 13 Exponential/Gaussian randomization for background/target using simulated image.

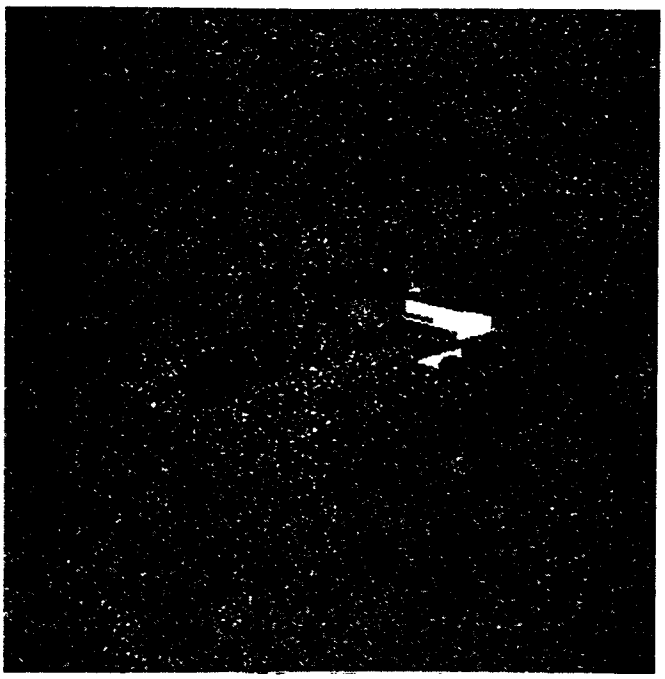

Figure 14 Gaussian/exponential randomization for background/target using simulated image.

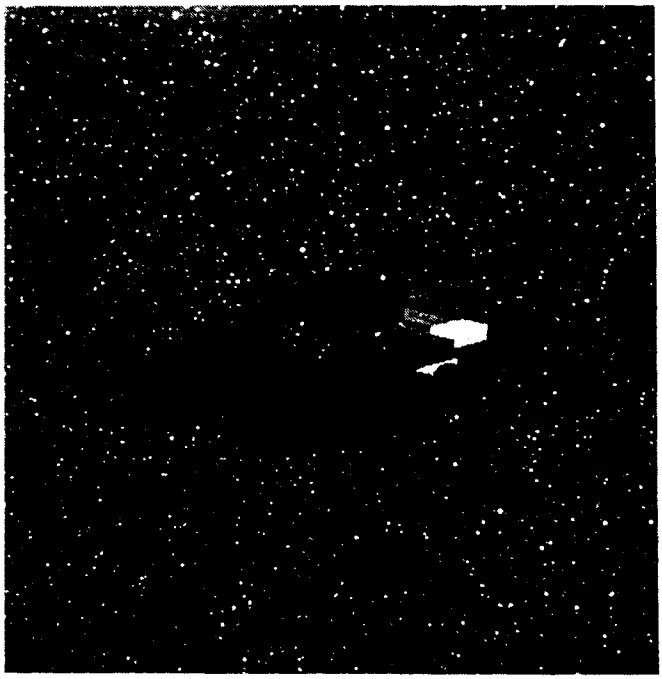

Figure 15 Log-normal/Rice randomization for background/target using simulated image.

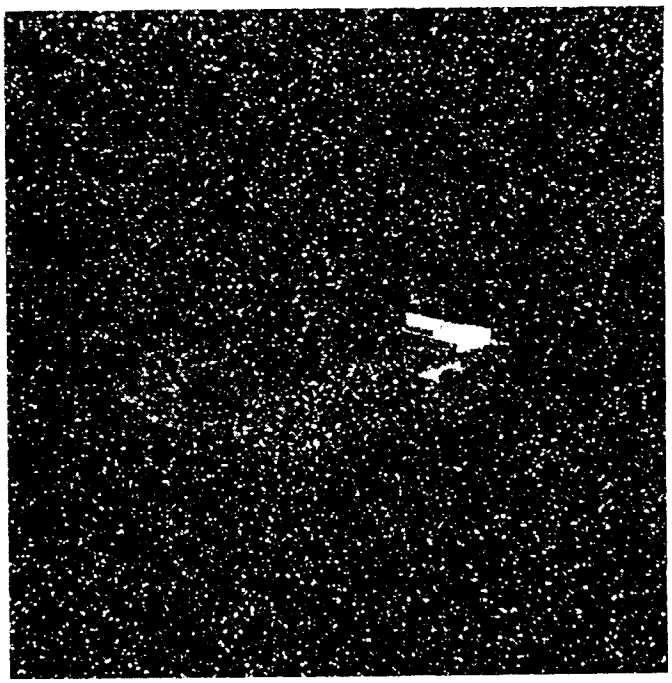

Figure 16 Rice/log-normal randomization for background/target using simulated image.

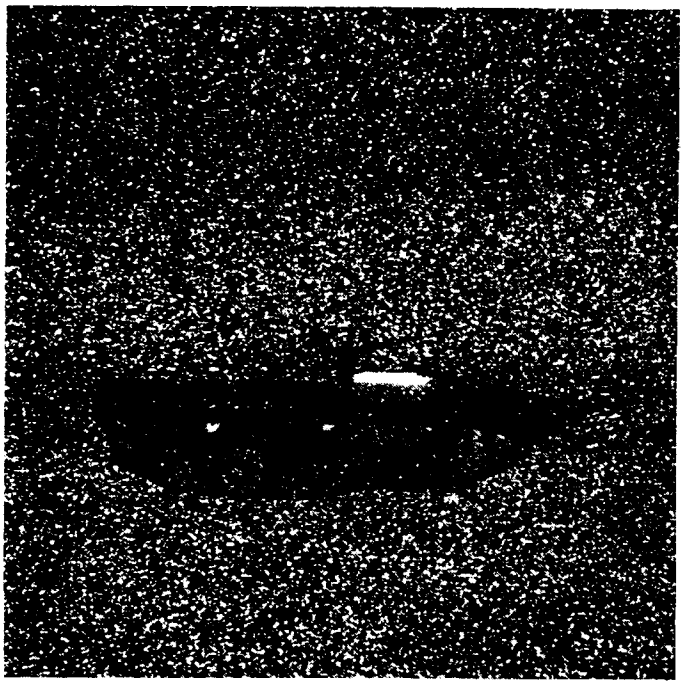

Figure 17 Exponential/log-normal randomization for background/target using measured image.

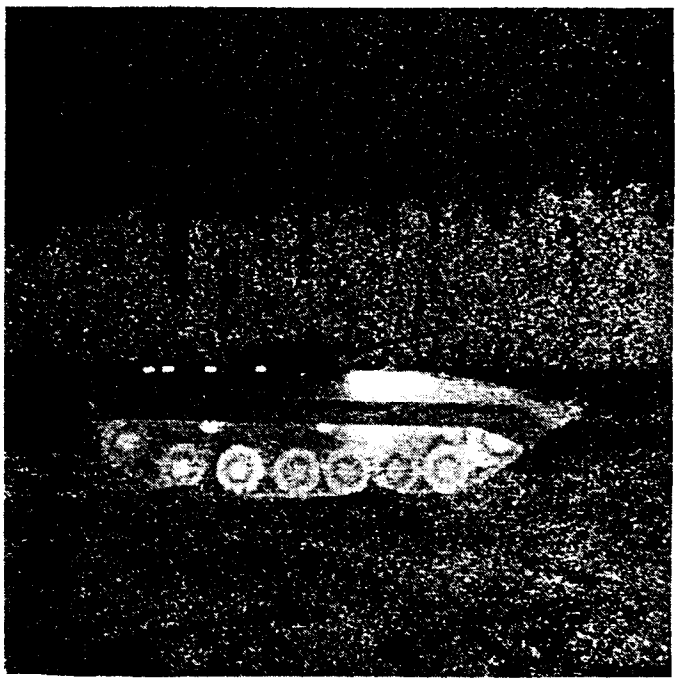

Figure 18 Gaussian/Rice randomization for background/target using measured image.

Figure 19 Log-normal/Gaussian randomization for background/target using measured image.

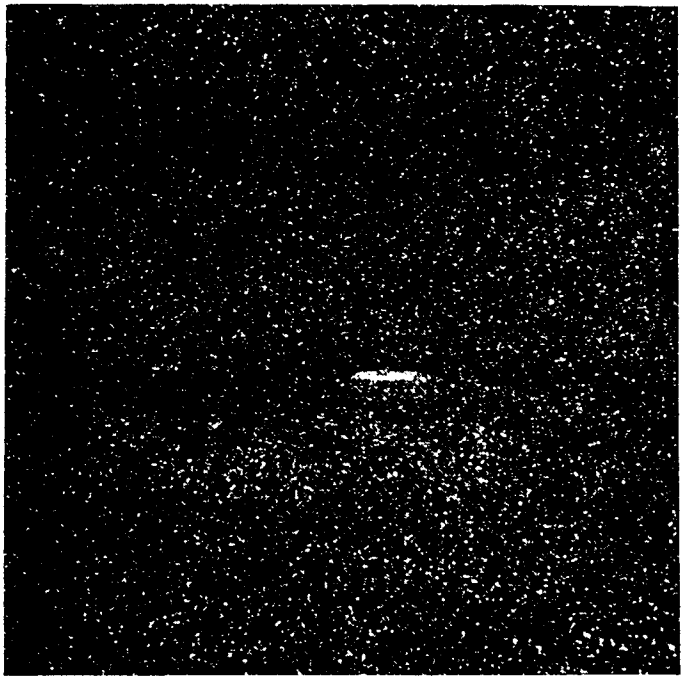

Figure 20 Rice/exponential randomization for background/target using measured image.

3. A NEW ΔT DEFINITION

In this section, a new ΔT metric definition is stated, and the equation based on this definition is derived. This definition is compared with other ΔT metric definitions such as the conventional ΔT (=AWA$\Delta\Delta T$), the Night Vision Laboratory (NVL) RMS ΔT in [2], and the ΔT found in [3]. The ΔT results from these various definitions are also compared by using Figures 13 - 20. The conventional ΔT, NVL ΔT, and the ΔT from [3] are denoted by ΔT_{conv}, ΔT_{NVL}, and $\Delta T_{[3]}$, respectively. The equations for ΔT_{conv}, ΔT_{NVL}, and $\Delta T_{[3]}$ are given in (13.a), (13.b), and (13.c), respectively.

$$\Delta T_{conv} = \mu_T - \mu_B \quad (a); \qquad \Delta T_{NVL} = \left[\frac{1}{N_T}\sum_{i=1}^{N_T}(P_i^T - \mu_T)^2\right]^{\frac{1}{2}} = \sigma_T \quad (b); \qquad \Delta T_{[3]} = \sqrt{(\mu_T - \mu_B)^2 + \sigma_T^2} \quad (c) \tag{13}$$

where, μ_T : The mean temperature of the target pixels
N_T : The number of pixels on target
σ_T : The standard deviation of the target pixel temperature
P^T : Each target pixel's temperature
μ_B : The mean temperature of the background pixels

The ΔT_{conv}, as shown in (13.a), does not consider temperature varying features on both target pixels and background pixels. This ΔT_{conv} definition is an oversimplification of the background and target temperature characteristics. The ΔT_{NVL} is simply a standard deviation of the target pixel temperatures. No background terms are involved in (13.b) indicating the background temperature is ignored. The $\Delta T_{[3]}$ considers the target temperature varying feature by having σ_T; however, the background temperature varying feature is not considered. It is evident in (13.b) and (13.c) that ΔT_{NVL} and $\Delta T_{[3]}$ cannot yield a negative ΔT, a case where the target is cooler than the background. These deficiencies indicate the need to define a new ΔT metric that includes higher order statistics of both background and target pixels' temperatures.

A human operator does not see a separate target or background, but rather sees both at the same time. Therefore, an overall scene, which includes the target and background, should be involved in defining a new ΔT metric. This is because when the overall scene is located far enough away such that the entire scene falls onto a pixel, only the mean temperature of the scene is realized. However, this mean temperature is produced not only by the background temperature but also by the target temperature. Therefore, it is adequate to imitate the human perception of the scene by evaluating the standard deviation of the target pixels' temperatures conditioned on the mean temperature of the scene (= $\sigma_{T|S}$), and by evaluating the standard deviation of the background pixels' temperatures conditioned on the mean temperature of the scene (= $\sigma_{B|S}$). Then, **a new ΔT metric is defined as the difference between the standard deviation of target pixel temperatures conditioned on the mean temperature of scene and the standard deviation of background pixel temperatures conditioned on the mean temperature of scene.** This is shown in (14).

$$\Delta T_{new} \triangleq \sigma_{T|S} - \sigma_{B|S} \tag{14}$$

3.1 Formulation of the new ΔT equation

Prior to formulating the new ΔT metric equation, the pixel temperature statistics of target/background and scene are expressed below. (15.a) and (15.b) show the mean and variance of the target pixel temperatures, respectively. The mean and variance of pixel temperatures on the background are expressed in (16.a) and (16.b), respectively.

$$\mu_T = \frac{1}{N_T}\sum_{i=1}^{N_T} P_i^T \quad (a); \qquad \sigma_T^2 = \frac{1}{N_T}\sum_{i=1}^{N_T}\left(P_i^T - \mu_T\right)^2 = \frac{1}{N_T}\sum_{i=1}^{N_T}\left(P_i^T\right)^2 - \mu_T^2 \quad (b) \tag{15}$$

$$\mu_B = \frac{1}{N_B}\sum_{i=1}^{N_B} P_i^B \quad (a); \qquad \sigma_B^2 = \frac{1}{N_B}\sum_{i=1}^{N_B}\left(P_i^B - \mu_B\right)^2 = \frac{1}{N_B}\sum_{i=1}^{N_B}\left(P_i^B\right)^2 - \mu_B^2 \quad (b) \tag{16}$$

where, P^T : Pixel temperature on target
σ_T^2 : The variance of pixel temperatures on target
μ_T : The mean of pixel temperatures on target
N_T : Number of pixels on target

P^B : Pixel temperatures on background
σ_B^2 : The variance of pixel temperatures on background
μ_B : The mean of pixel temperatures on background
N_B : Number of pixels on background

The mean and variance of the overall scene are given in (17.a) and (17.b), respectively. It is noted that $N_S = N_B + N_T$.

$$\mu_S = \frac{1}{N_S}\sum_{i=1}^{N_S} P_i^S = \frac{\mu_T N_T + \mu_B N_B}{N_T + N_B} \qquad (a)$$

$$\sigma_S^2 = \frac{1}{N_S}\sum_{i=1}^{N_S}\left(P_i^S - \mu_S\right)^2 = \frac{1}{N_S}\sum_{i=1}^{N_S}(P_i^S)^2 - \mu_S^2 = \frac{\left(\sigma_T^2 + \mu_T^2\right)\times N_T + \left(\sigma_B^2 + \mu_B^2\right)\times N_B}{N_T + N_B} - \left(\frac{\sum_{i=1}^{N_T} P_i^T - \sum_{i=1}^{N_B} P_i^B}{N_T + N_B}\right)^2 \qquad (b) \qquad (17)$$

where, P^S : Pixel temperatures on scene
μ_S : The mean of pixel temperatures on scene

σ_S^2 : The variance of pixel temperatures on scene
N_S : Number of pixels on scene ($= N_B + N_T$)

Then, $\sigma_{T|S}^2$ and $\sigma_{B|S}^2$ can be expressed in terms of μ_T, σ_T, N_T, μ_B, σ_B, N_B, and N_S. The conditional variances are shown in (18.a) and (18.b) for the target and background pixel temperatures, respectively.

$$\sigma_{T|S}^2 = \frac{1}{N_T}\sum_{i=1}^{N_T}\left(P_i^T - \mu_S\right)^2 = \sigma_T^2 + \mu_T^2 - 2\mu_T\mu_S + \mu_S^2 = \frac{1}{N_S^2}\left[N_S^2\times\sigma_T^2 + N_B^2\times\left(\mu_T - \mu_B\right)^2\right] \qquad (a)$$

$$\sigma_{B|S}^2 = \frac{1}{N_B}\sum_{i=1}^{N_B}\left(P_i^B - \mu_S\right)^2 = \sigma_B^2 + \mu_B^2 - 2\mu_B\mu_S + \mu_S^2 = \frac{1}{N_S^2}\left[N_S^2\times\sigma_B^2 + N_T^2\times\left(\mu_B - \mu_T\right)^2\right] \qquad (b) \qquad (18)$$

Therefore, the new ΔT metric equation ($= \Delta T_{new}$) is the difference between the square root of (18.a) and the square root of (18.b). This is written in (19).

$$\Delta T_{new} = \sigma_{T|S} - \sigma_{B|S} = \frac{1}{N_S}\left[\sqrt{N_S^2\sigma_T^2 + N_B^2\times\left(\mu_T - \mu_B\right)^2} - \sqrt{N_S^2\sigma_B^2 + N_T^2\times\left(\mu_B - \mu_T\right)^2}\right] \qquad (19)$$

In the above equation, it is apparent that the temperature varying feature on the target and background pixels is included in terms of their variances. Also, the number of pixels on target, background, and scene is also included, which shows (19) is a pixel-based temperature difference between the target and background. Of course, the mean temperatures of the target and background are also present in (19).

3.2 Comparison of ΔT_{new} metric to other ΔT metric equations

The other ΔT metric equations introduced earlier (ΔT_{conv}, ΔT_{NVL}, and $\Delta T_{[3]}$) will now be compared to the ΔT_{new} metric. The ΔT_{conv} metric is evaluated by the mean temperatures of the target and background as shown in (13.a). It ignores temperature variations of the target and background pixels. Thus, the variances of the target and background are zero, $\sigma_T^2 = \sigma_B^2 = 0$. Under these conditions, the ΔT_{new} metric reduces to in the ΔT_{conv} metric as shown in (20).

$$\Delta T_{new}\big|_{\sigma_T=0,\sigma_B=0} = \frac{1}{N_S}\left[N_B\times\left(\mu_T - \mu_B\right) - N_T\times\left(\mu_B - \mu_T\right)\right] = \frac{1}{N_S}\times\left(N_T + N_B\right)\times\left(\mu_T - \mu_B\right) = \mu_T - \mu_B = \Delta T_{conv} \qquad (20)$$

The ΔT_{NVL} metric, as mentioned before, is simply a standard deviation of the target pixel temperatures as shown in (13.b). It does not consider any background characteristics nor the mean target temperature. These conditions can be written such as $\mu_B = \sigma_B = N_B = \mu_T = 0$. Under these conditions, the ΔT_{new} metric reduces to the ΔT_{NVL} metric as shown in (21).

$$\Delta T_{new}\Big|_{\substack{\mu_B=0,\sigma_B=0\\ N_B=0,\mu_T=0}} = \sigma_T = \Delta T_{NVL} \tag{21}$$

The $\Delta T_{[3]}$ metric, from the equation shown in (13.c), considers the temperature variance on target pixels but not on background pixels. It also considers the mean temperature of the target and background as the ΔT_{conv} metric. This condition can be written as $\sigma_B = 0$, which means a uniform background. For this condition, the ΔT_{new} metric becomes (22).

$$\Delta T_{new}|_{\sigma_B=0} = \frac{1}{N_S}\left[\sqrt{N_S^2\,\sigma_T^2 + N_B^2(\mu_T - \mu_B)^2} - N_T(\mu_B - \mu_T)\right] \tag{22}$$

It seems that there is no direct relationship between (22) and the $\Delta T_{[3]}$ metric unless some special conditions are considered. If the mean of the target and background pixel temperatures are the same ($\mu_T = \mu_B$), (13.c) and (22) become the standard deviation of the pixel temperatures on the target only, which is the ΔT_{NVL} metric as shown in (23).

$$\Delta T_{new}|_{\sigma_B=0,\mu_T=\mu_B} = \Delta T_{[3]}|_{\mu_T=\mu_B} = \Delta T_{NVL} = \sigma_T \tag{23}$$

If the variance of the target pixel temperatures (σ_T^2) is zero, i.e., a uniform target temperature, (13.c) and (22) become the difference between the target mean temperature and the background mean temperature. Thus, in this case, ΔT is the ΔT_{conv} metric as shown in (24).

$$\Delta T_{new}|_{\sigma_B=0,\sigma_T=0} = \Delta T_{[3]}|_{\sigma_T=0} = \Delta T_{conv} = \mu_T - \mu_B \tag{24}$$

Therefore, the ΔT_{conv}, ΔT_{NVL}, and $\Delta T_{[3]}$ metrics describe special cases of the ΔT_{new} metric. The ΔT_{new} metric given in (19) includes various effects due to the target and background characteristics in a temperature scene image by evaluating a number of pixels on the target and the background, the mean of the target and background temperatures, and the variance of the target and background temperatures. The variance represents the temperature varying feature of the target and background. The ΔT_{new} metric is derived from a conditional standard deviation of the target and background pixel temperatures on an overall scene as shown in (18.a), (18.b), and (19). However, the other ΔT metrics are derived by evaluating the target and the background separately as if they belong to separate images. This is not a correct interpretation of the image under evaluation, since an operator views the target pixels and background pixels in the evaluated image simultaneously.

3.3 ΔT_{new} metric comparison with other ΔT metrics using Figures 13 through 20

Figures 13 - 20 are used to obtain ΔT values using the ΔT_{conv}, ΔT_{NVL}, $\Delta T_{[3]}$, and ΔT_{new} metric equations given by (13.a), (13.b), (13.c), and (19), respectively. Table 4 lists the target and background statistics and ΔTs of Figures 13 - 16. Table 5 shows the same for Figures 17 - 20.

Using images in Figures 13 - 16, the various ΔT definitions discussed in Sections 3.0, 3.1, and 3.2 were evaluated. All of the target and the background pixels contributed to the ΔT results. Observing Figure 13 and its ΔT values, it is difficult to tell which ΔT represents Figure 13. Nevertheless, the ΔT above 10 degrees Kelvin seems too high compared to Figure 13. The ΔT_{new} seems to be an adequate result for Figure 13. In Figure 14, the background mean temperature and the target mean temperature were intentionally matched using BATRAN to evaluate the performance of each ΔT metric. As seen in Figure 14, much of the target features are buried in the background due to the matching. The ΔT_{conv} is zero, which is not a true statement because the target can still be detected and recognized. The ΔT_{NVL} and $\Delta T_{[3]}$ may be reasonable only if hot parts of the target are considered. Since all of the target pixels were considered in evaluating ΔT, the results from these definitions may not properly describe the image. The result from the ΔT_{new} metric provides a more correct representation for the image. In Figure 15, not only were the background mean temperature and target mean temperature closely matched, but also the background variance and the target variance were closely matched using BATRAN. As seen in Figure 15, the target image is deteriorating. Except for a few hat parts, most of the target parts are relatively cooler than the background. The results from the ΔT_{NVL} and $\Delta T_{[3]}$ metrics are only the standard deviation

(σ) of the target pixel temperatures, and the results from these metrics are relatively high compared to the image. The ΔT_{new} and ΔT_{conv} values are very close to each other. This is because the variance of the background and the target pixels were matched. These results may not reflect target recognition ability. In Figure 15, human eyes can easily detect and recognize the target. The ΔT results using the image depicted in Figure 16 show that the ΔT_{conv}, ΔT_{NVL}, and $\Delta T_{[3]}$ values are too high, all being greater than 12 degrees Kelvin. The ΔT_{new} value shows a reasonable result for the image.

Table 4 Simulated image output pixel statistics and various ΔTs comparison.

Simulated image	Background pixel statistics (N_B= 130447)		Target pixel statistics (N_T = 12059)		Temperature Difference (ΔTs)			
Figure #	μ_B	σ_B	μ_T	σ_T	ΔT_{conv}	ΔT_{NVL}	$\Delta T_{[3]}$	ΔT_{new}
13	285.01	101.09	294.46	135.76	9.45	11.65	15.0	4.42
14	299.46	25.58	299.46	60.20	0.00	7.76	7.76	2.70
15	295.51	36.65	295.54	37.26	0.03	6.10	6.10	0.05
16	290.55	227.60	306.30	149.72	15.75	12.24	12.24	3.77

Table 5 Measured image output pixel statistics and various ΔTs comparison.

Measured image	Background pixel statistics (N_B= 239731)		Target pixel statistics (N_T = 22413)		Temperature Difference (ΔTs)			
Figure #	μ_B	σ_B	μ_T	σ_T	ΔT_{conv}	ΔT_{NVL}	$\Delta T_{[3]}$	ΔT_{new}
17	311.33	678.10	311.34	186.47	0.01	13.66	13.66	-12.39
18	296.34	154.06	314.37	166.23	18.03	12.89	22.77	8.42
19	296.34	134.24	297.30	124.96	0.965	15.59	15.62	4.03
20	320.38	1096.38	333.98	1004.32	13.60	31.69	34.48	0.91

Using images in Figures 17 - 20, the various ΔT metrics are also discussed. The background mean temperature and the target mean temperature are closely matched using BATRAN in Figure 17. This results in ΔT_{conv} close to zero. The ΔT_{NVL} and $\Delta T_{[3]}$ values are the standard deviation of the target pixel temperatures, and their results are too high compared to Figure 17. The overall target temperature is cooler than the overall background. This is shown in ΔT_{new} with a negative value. As previously noted in Section 3.0, the ΔT_{NVL} and $\Delta T_{[3]}$ metrics cannot discern whether the background is cooler than the target, or vice versa. Figure 18 closely represents the image taken during 30 mm/hour rain fall.* The BATRAN randomization can be used to generate images which may represent the target and background under various weather conditions. The ΔT results from Figure 19 show that the ΔT_{NVL} and $\Delta T_{[3]}$ values are too high compared to the image. Either ΔT_{conv} or ΔT_{new} value represents a reasonable temperature difference between the background and the target. The ΔT results calculated from Figure 20 clearly tell the tolerance of each ΔT metric. The image may represent the background and the target under a severe weather condition. The target is barely distinguishable in the image. However, the ΔT_{conv}, ΔT_{NVL}, and $\Delta T_{[3]}$ metrics yield the temperature differences of 13.6, 31.69, 34.48 degrees Kelvin, respectively. These unreasonable results were found because the definition of these metrics considers the target and the background separately as if they belong to separate images. Also, these definitions do not consider the background temperature varying features in their equations. However, the ΔT_{new} metric interpreted the image under a severe weather condition, as shown in Figure 20, quite well.

4. SUMMARY AND CONCLUSIONS

Background, clutter, and target field measurements from EO/IR, ladar (laser radar), visual, and other sensor systems show their statistics can be represented by the distributions implemented in the BATRAN (Background and Target Randomization) software, namely exponential, Gaussian, log-normal, and Rice distributions. The background and target pixel randomization algorithm using these distributions was first developed analytically prior to implementation in the BATRAN software, which performs the randomization on an input scene image. The background can be randomized by a statistical distribution which differs from the target randomizing statistical distribution. Also, background and target randomizing statistical distributions may be the same. The BATRAN software allows for insertion of randomness, which may represent artifacts due to aliasing, background characteristics, and varying amounts of clutter, into sensor images. The randomness is produced according to the given statistical distributions so that the randomized image can be used to

* Figure 18 was compared to a real image taken by TARDEC during 30 mm/hr rain fall.

analyze various detection and ATR algorithms. BATRAN is also able to incorporate weather effects on sensor image if the weather statistical characteristics are known. With these capabilities, BATRAN is a tool for enhancing the effectiveness assessment of signature management technologies for military ground vehicles, thus increasing their survivability.

The background RMS matching with a target was performed with a newly developed ΔT metric definition. This new ΔT metric, denoted by ΔT_{new} in this paper, performed better than the other definitions reviewed in this paper when applied to various scene images, both simulated and measured. Once the background/clutter and target statistics are known, and can be described any one of the BATRAN implemented statistics, the BATRAN software can match the target signature to the background/clutter well by adjusting the given target and/or background statistical parameters to provide a desired temperature difference (ΔT). Various combinations of background/clutter and target statistics generated the output images (Figures 13 - 20) from the input scene images (Figures 11 and 12). These output images indicate each combination's ability to match a target to the background/clutter to a human observer. Using the ΔT_{new} metric, the target and background can be matched not only in their mean temperatures but also in their temperature varying features, i.e., variance or standard deviation. This corrects the deficiencies of the existing ΔT metrics mentioned in Section 3.0. It was also concluded that the ΔT_{new} metric gave the best apparent match of the suppressed vehicle with the background.[9] Therefore, the ΔT_{new} metric allows for a more robust and accurate assessment of the detection performance of thermal imaging systems than the other ΔT metrics.

5. ACKNOWLEDGEMENTS

This work was supported by Dr. Grant Gerhart at the U.S. Army Tank Automotive Research, Development and Engineering Center (TARDEC) under the auspices of the U.S. Army Research Office Scientific Services Program administered by Battelle (Delivery Order 509, Contract No. DAAL03-91-C-0034). Mr. Thomas Meitzler of TARDEC served as technical monitor for the material presented herein.

6. REFERENCES

[1] James A. Ratches, *Static Performance Model for Thermal Imaging Systems*, Optical Engineering, Nov.-Dec. 1976, Vol. 15, No. 6, pp525-530.

[2] "Step 1: Metric Quantification for Characterizing Target Thermal Contrast and Dimension," Visionics Modeling Division, Night Vision and Electro Optics Directorate, July 29, 1992.

[3] Michael R. Whalen and Eric J. Borg, *The Thermal Contrast Definition for Infrared Imaging Sensors*, Dynetics, Inc.

[4] Milton Abramowitz and Irene A. Stegun, "Handbook of Mathematical Functions with Formulas, Graphs, and Mathematical Tables," National Bureau of Standards, U. S. Department of Commerce, U.S. Government Printing Office, Washington D. C., 1972.

[5] Howard C. Choe, James G. McGraw, and Philip G. Tomlinson, "Bistatic Radar Detection in Clutter - Phase II, Final Report," Decision-Science Application, Inc., DSA Report 39/1174, 1990.

[6] Merrill I. Skolnik, "Introduction to Radar Systems-Second Edition," McGraw-Hill Book Company, 1980.

[7] Albert V. Jelalian, "Laser Radar Systems," Artech House, Boston, 1992.

[8] William H. Press, Brian P. Flannery, Saul A. Teukolsky, and William T. Vetterling, "Numerical Recipes-The Art of Scientific Computing," Cambridge University Press, Printed in New York, New York, 1986.

[9] Grant R. Gerhart, Thomas J. Meitzler, Sanjiv Dungrani, and Howard C. Choe, *Evaluation of ΔT using statistical characteristics of the target and background*, SPIE Proceedings Vol. 1967, April 1993.

[10] Athanasios Papoulis, "Probability, Random Variables, and Stochastic Processes-Second Edition," McGraw-Hill Book Company, New York, New York, 1984.

[11] Samuel S. Wilks, "Mathematical Statistics," John Wiley & Sons, Inc., New York, New York, 1962.

[12] J. M. Lloyd, "Thermal Imaging Systems," Plenum Press, New York, New York, 1982.